

Lu-Hf AND Sm-Nd ISOTOPIC STUDIES OF NAKHLITE NORTHWEST AFRICA 10153. M. Righter¹, T. J. Lapen¹, R. Andreasen^{1,2}, and, A. J. Irving³, ¹Department of Earth and Atmospheric Science, University of Houston, Houston TX 77204-5007 (mrighter@uh.edu), ²Dept. of Geoscience, Aarhus University, Denmark. ³Dept. of Earth and Space Sciences, University of Washington, Seattle, WA 98195.

Introduction: Nakhrites are unbrecciated, olivine-bearing Martian clinopyroxenites consisting of cumulus augite and olivine as well as intercumulus phases. All nakhrites have been only moderately shocked and their original igneous textures are still well preserved [e.g., 1]. A total of nine nakhrites have been identified including three recent finds: MIL 090030/090032/090136, NWA 5790 and NWA 10153. Nakhrites show petrographical and mineralogical variations that have been explained by different locations (burial depths) in a common cooling cumulus pile [2-4]. The radiometric ages of the nakhrites are generally well-constrained at ~1.35 Ga and these meteorites also have concordant ejection ages [5, 6], suggesting that they might have been ejected from the same place on Mars by the same impact event. In this study, we present Sm-Nd and Lu-Hf isotope and trace element data for NWA 10153. We place these in the context of existing Sm-Nd and Lu-Hf data of nakhrites with the aim of identifying similarities and potential source affinities among nakhrites.

Petrology & Mineralogy of NWA 10153: NWA 10153 is mainly composed of augite with olivine set in a mesostasis (Fig. 1). Augite is euhedral and prismatic reaching up to 2.2 mm long, having large homogeneous magnesian cores ($\text{En}_{37}\text{Fs}_{23}\text{Wo}_{40}$) with higher Fe contents ($\text{En}_{37}\text{Fs}_{23}\text{Wo}_{40} \sim \text{En}_{15}\text{Fs}_{45}\text{Wo}_{40}$) at the rim. Augite in the mesostasis has lower Wo contents ($\text{En}_{18}\text{Fs}_{50}\text{Wo}_{32}$). Olivine is euhedral to subhedral and extensively zoned (Fa_{61-84}). Olivine cores contain ~0.5 wt% CaO, decreasing to ~0.1 wt% at the rim. Magmatic inclusions were found in both augite and olivine. The mesostasis is composed of plagioclase ($\text{An}_{18-26}\text{Or}_{5.7-3.1}$), K-rich feldspar, titanomagnetite with ilmenite exsolution, pyroxene, olivine, silica mineral and Ca phosphate [7].

Samples and Analytical Procedures: A polished slab was analyzed for trace element abundances in the major constituent phases by LA-ICPMS at the University of Houston. The abundances of Nd and Hf were used to estimate the amount of spike needed for isotopic analyses. A ~1 g aliquot of NWA 10153 was crushed with an alumina mortar and pestle. The crushed material was sieved into various size fractions, of which the finest grain size fractions (<44 μm) were used for whole rock analyses (WR1, WR2, and WR3). The 100-200 and 200-325 mesh fractions were used for further mineral separations by density separation

using heavy liquids of 2.96 and 4.05 g/cm^3 . The $2.96 < \rho < 4.05 \text{ g}/\text{cm}^3$ fraction was further separated into pyroxene- and olivine-rich fractions using a Frantz magnetic separator. At 0.2 ampere, we obtained a pyroxene sample from the less-magnetic fraction. All mineral fractions were further purified by handpicking. A total of five mineral fractions were isolated: two pyroxene fractions (Px1, Px2), olivine, oxide (Ox), and a plagioclase-rich fraction ($\rho < 2.96$; Plag). All chemical separation procedures were carried out in clean lab facilities at University of Houston and NASA Johnson Space Center, and all isotope analyses were carried out using the Nu Plasma II MC-ICP-MS at the University of Houston.

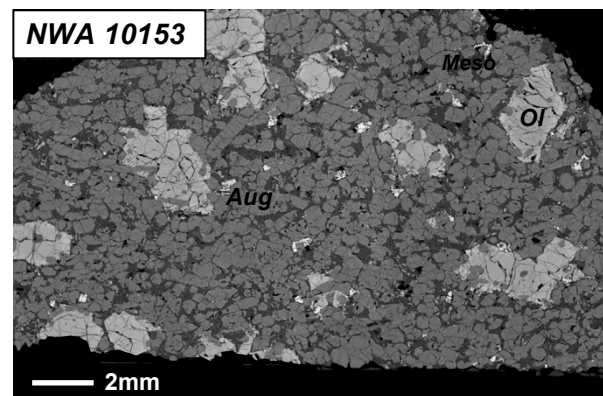


Figure 1. Backscattered electron image of NWA 10153. Aug: augite. Ol: olivine. Meso: mesostasis.

Results: Rare Earth Element (REE) Concentrations: The chondrite-normalized REE abundances of the primary phases (augite, olivine, and plagioclase) are presented in Figure 2. Chondrite-normalized REE abundances of augite increase smoothly from La to Nd and, thereafter, the REE pattern slopes slightly downwards. This pattern is characteristic of high-Ca pyroxenes in the nakhrites [8]. The plagioclase REE pattern decreases from LREE to MREE and is nearly flat afterwards with a positive Eu anomaly. Nd, Sm and Lu concentrations of all three primary phases are lower than those of the whole rock, suggesting that Ca-phosphate is the main host of REE.

Sm-Nd isotopic results: $^{147}\text{Sm}/^{144}\text{Nd}$ and $^{143}\text{Nd}/^{144}\text{Nd}$ data of 8 samples of NWA 10153 are shown in Fig. 3. One pyroxene (Px1), two whole rock (WR1 and WR2) and two acid-residues (Px2(r), Plag(r)) define a linear array corresponding to a Sm-

Nd age of 1419 ± 56 Ma (MSWD = 0.57) for $\lambda(^{147}\text{Sm}) = 0.00654 \text{ Ga}^{-1}$ with an initial $^{143}\text{Nd}/^{144}\text{Nd}$ value of 0.511518 ± 0.000054 using the Isoplot regression program [9]. Three leachate samples (Px2(l), WR3(l) and Plag(l)), and one residue sample from the fine grained cut (WR3(r)), lie off the isochron, and probably contain secondary alteration products. Our best estimate Sm-Nd age for NWA 10153 is in good agreement with those for other nakhlites [10-14]. The initial $\epsilon^{143}\text{Nd}$ value for NWA 10153 is $+13.8 \pm 1.0$. The initial $\epsilon^{143}\text{Nd}$ for other nakhlites are: Nakhla ($+16.2$) [14], MIL 03346 ($+16.1$) [13] and Y000593 ($+16.9$) [12] as well as initial obtained by mineral isochron for Governador Valadares ($+16.7$) [11], Lafayette ($+16.3$) [10], MIL 03346 ($+15.2$), Nakhla ($+16.8$) [14], NWA 5790 ($+15.4$) [14]. The $\mu^{142}\text{Nd}$ for NWA 10153 is $+53.2 \pm 6.6$ (95% confidence) and is lower than the average value of $+63$ for Nakhla, MIL 03346, and Y000593 [15].

Lu-Hf isotopic results: $^{176}\text{Lu}/^{177}\text{Hf}$ and $^{176}\text{Hf}/^{177}\text{Hf}$ data of four samples of NWA 10153 are shown in Fig. 4. Two whole rock (WR1 and WR2), pyroxene (Px1) and oxide fraction (Ox) form a linear array corresponding to an age of 1360 ± 33 Ma (MSWD = 0.53) for $\lambda(^{176}\text{Lu}) = 1.865 \times 10^{-11} \text{ yr}^{-1}$ with an initial $^{176}\text{Hf}/^{177}\text{Hf}$ value of 0.282009 ± 0.000016 . This is the first mineral Lu-Hf isochron obtained from a nakhlite, and is in agreement with the $^{147}\text{Sm}-^{144}\text{Nd}$ age obtained from the same sample aliquots. The initial $\epsilon^{176}\text{Hf}$ value for NWA 10153 is $+3.4$, which is significantly lower than previously published nakhlite data (Nakhla: $+13.5$; MIL 003346: $+12.6$, Y000593: $+19.7$) [15].

Discussion: The isochron ages of NWA 10153 agree well with published ages, suggesting that the suite of nakhlites are derived from the same (or similar) magmatic system. The initial isotope compositions and $\mu^{142}\text{Nd}$ could suggest variable mantle sources, with NWA 10153 being derived from more enriched components. Alternatively, assimilation of crustal material during magma ascent and emplacement could also explain the more enriched initial isotope values. The latter scenario could be consistent with petrographic observations of late stage igneous water-bearing minerals in NWA 10153 [7]. Further tests are required to evaluate these hypotheses.

References: [1] Treiman A. (2005) *Chemie der Erde*, 65, 203–270. [2] Mikouchi T. et al. (2003) *Antarct. Meteorite Res.*, 16, 34–57. [3] Mikouchi T. et al. (2006) *LPS XXXVII*, Abstract 1865. [4] Mikouchi T. et al. (2012) *LPS XLIII*, Abstract 2363. [5] Nyquist L.E. et al. (2001) *Chronology and Evolution of Mars*, 105–164. [6] Busemann H. et al. (2015) *Meteoritics & Planet. Sci.*, 50, Abstract 5235. [7] Irving A. J. et al. (2015) *Meteoritics & Planet. Sci.*, 50, Abstract 5251. [8] Wadhwa M. and Crozaz G. (1995) *GCA* 59, 3629–3645.

[9] Ludwig K. R. (2012) *Berkeley Geochronology Center Spec. Pub.* 1a, 59. [10] Shih C.-Y. et al. (1998) *LPS XXIX*, Abstract 1145. [11] Shih C.-Y. et al. (1999) *Meteoritics & Planet. Sci.*, 34, 647–655. [12] Misawa K. et al. (2005) *Antarct. Meteorite Res.* 18, 133–151. [13] Shih C.-Y. et al. (2006) *LPS XXVII*, Abstract 1701. [14] Shih C.-Y. et al. (2010) *LPS XLI*, Abstract 1367. [15] Debaille V. et al. (2009) *Nature Geoscience*, 2, 548–552.

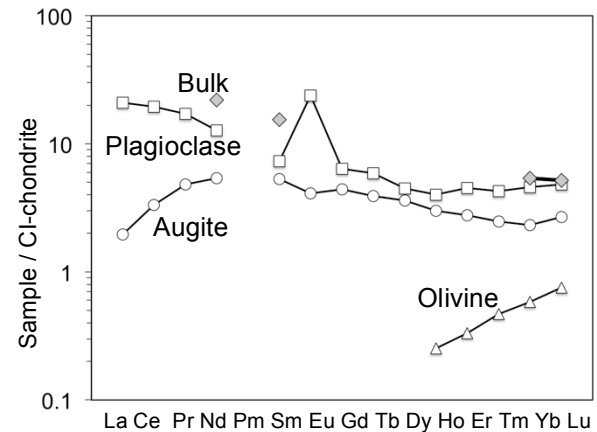


Figure 2. Mineral REE compositions in NWA 10153.

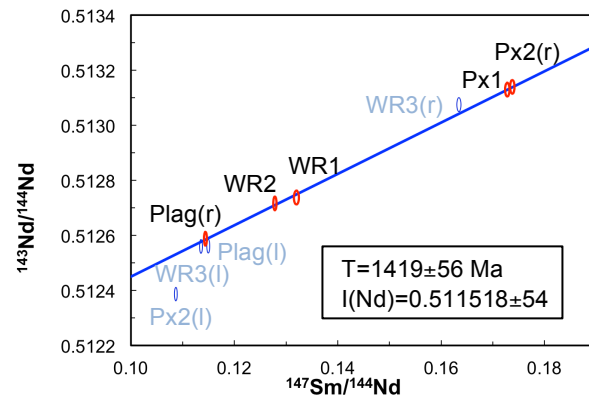


Figure 3. Sm-Nd data for NWA 10153.

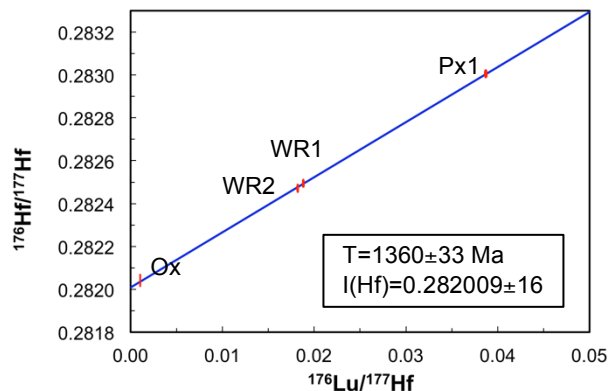


Figure 4. Lu-Hf data for NWA 10153.